DNS OF THE INTERACTION BETWEEN A SHOCK WAVE AND A TURBULENT SHEAR FLOW: SOME EFFECTS OF ANISOTROPY

Matthieu Crespo and Stéphane Jamme
Fluid Mechanics Department, ENSICA
1 Place Emile Blouin, 31056 Toulouse cedex 5, France
mcrespo@ensica.fr, jamme@ensica.fr

Patrick Chassaing
Institut de Mécanique des Fluides de Toulouse,
Allée du Professeur Camille Soula, 31400 Toulouse, France
Patrick.Chassaing@imft.fr

ABSTRACT

Direct numerical simulation is used to study the interaction of a Mach 1.5 shock wave and various types of anisotropic turbulent flows at $Re_\lambda = 47$. We compare the interaction of isotropic, axisymmetric and sheared turbulences (sometimes combined), with a specific interest for the sheared situation. The sign and magnitude of the correlation between the velocity and temperature fluctuations are found to have a crucial influence on the kinetic energy amplification across the shock. A decrease in magnitude is observed during the interaction for the velocity cross-correlation $\widetilde{u''v''}$. The balance equation of this quantity is investigated and the terms responsible for this behaviour are identified. The shear stress effect upon fluctuating vorticity and the dissipation length scale is also presented. Thermodynamic fluctuations are finally analyzed, showing the departure from the isentropic state in the sheared situation compared to the isotropic one.

INTRODUCTION

The interaction of free isotropic turbulence with a normal shock wave has been the focus of several studies in the past ten years. The first ones were theoretical works that relied on linear analysis and Kovasznay's modal decomposition of turbulence (Kovasznay, 1953). They developed the so-called Linear Interaction Analysis (LIA) (Ribner, 1953) which was recently revisited and completed by Mahesh *et al.* (1997) and Fabre *et al.* (2001) for instance. Experimental research has also been conducted using shock tubes and wind tunnels (see *e.g.* Agui *et al.* (2005) for a review). More recently, Direct Numerical Simulations (DNS) and Large Eddy Simulations (LES) of shock-turbulence interaction began to emerge (see *e.g.* Jamme *et al.*, 2002). All the works cited above allowed to understand the main features of shock-turbulence interaction when the upstream turbulent flow is isotropic.

However, the influence of anisotropy on the interaction has seldom been investigated. Mahesh *et al.* (1994) used Rapid Distortion Theory (RDT) to study the response of anisotropic turbulence to rapid homogeneous 1D compression, and Jamme *et al.* (2005) used DNS to characterize the behaviour of an axisymetric turbulent flow through the shock wave. The purpose of the present work is to investigate how the presence of an idealized mean shear upstream of the shock may modify the interaction phenomenon compared to axisymmetric cases where no shear was present. We investigate the behaviour of the main turbulent statistics of the flow during the interaction.

NUMERICAL METHOD

We solve the full three-dimensional Navier-Stokes equations in non-dimensional conservative form using a finite difference approach. The inviscid part is resolved using a fifth-order Weighted Essentially Non-Oscillatory scheme (WENO : Ponziani *et al.*, 2003). Viscous terms are computed using a sixth-order accurate compact scheme (Lele, 1992). A fourth-order Runge Kutta algorithm (Jiang & Shu, 1996) is used to advance in time.

Equations are solved on a cubic domain of size 2π in the three directions (see Figure 1) and a grid of $176 \times 128 \times 128$ is used. The mean flow is aligned with x. Periodic conditions are specified in the z direction, and non-reflecting boundary conditions of Poinsot and Lele (1992) along with a sponge layer are used for the top and bottom boundaries along y, as well as for the outflow where the flow is subsonic. At the beginning of the calculation, a plane shock wave at Mach number M_1 is specified in the middle of the computational domain; the flow is steady on each side of the shock, satisfying the Rankine-Hugoniot relations.

At each time step, velocity, pressure, temperature, and density fields are specified at the inflow. These fields are superpositions of a supersonic mean flow and turbulent fluctuations (denoted further by a prime) in velocity, pressure, temperature, and density. The mean velocity at the inflow varies linearly across streamlines while the mean pressure is uniform. The mean temperature and density vary such as the mean Mach number is uniform :

$$\overline{U}_1(y) = U_0 + S(y - y_{\min}), \quad \overline{V}_1 = \overline{W}_1 = 0,$$
$$\overline{P}_1(y) = 1/(\gamma M_r^2), \quad \overline{T}_1(y) = M_r^2 U_1^2 / M_1^2,$$

where the overbar denotes the conventional Reynolds average and the subscript 1 indicates the upstream state. The shear stress magnitude is controled by the parameter S where $S = \partial\overline{U}_1/\partial y$. Turbulent fluctuations are then superposed onto the mean upstream flow and advected through the inflow boundary using Taylor's hypothesis. The anisotropy of the turbulent velocity fluctuations used in the inflow plane is typical of a turbulent shear flow. These fluctuations come from preliminary runs of freely evolving turbulence conducted in a cubic domain of $(2\pi)^3$ discretized

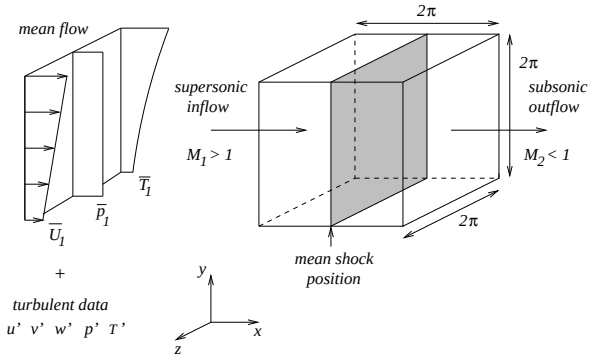

Figure 1: Flow configuration.

with an equidistant grid of 128^3 points. These simulations are initialized with a random velocity field. This field does not satisfy the Navier-Stokes equations, but

- its mean is aligned with x and equals $\overline{U}_1 = U_0 + S(y - y_{\min})$;
- the spectrum of the fluctuation is defined by

$$E(k) = 16\sqrt{\frac{2}{\pi}}\frac{u_0^2}{k_0}\left(\frac{k}{k_0}\right)^4 \exp\left[-2\left(\frac{k}{k_0}\right)^2\right],$$

  where u_0 is the rms value of any of the components of the fluctuation and $k_0 = 4$ the value of most energetic wave number (linked, for this spectrum, with the value of the Taylor microscale by $k_0 = 2/\lambda_0$);
- the fluctuating field ($\mathbf{u}$) is the sum of a divergence-free (rotational) field ($\mathbf{u}_s$) and a dilatational (irrotational) field ($\mathbf{u}_c$), the ratio (χ) of the dilatational to total turbulent kinetic energy being freely adjustable.

The random velocity field with constant pressure and density is used as an initial condition for the simulation of time-evolving turbulence in the cubic domain. Periodic boundary conditions are used in the x and z directions, whereas non-reflecting boundary conditions with sponge layers are used along y. Time evolution is stopped after the fluctuating fields are stabilized to a mean velocity derivative skewness ($Sk = (Sk_1 + Sk_2 + Sk_3)/3$, with $Sk_\alpha = \overline{(\partial u'_\alpha/\partial x_\alpha)^3}/[\overline{(\partial u'_\alpha/\partial x_\alpha)^2}]^{3/2}$) of -0.45 that makes them reasonably representative of real turbulence, and when the desired amount of turbulent kinetic energy (to feed the interaction runs) has been reached ($q^2/2 = 1.5$ in our cases).

DNS of the interaction of a shock wave with isotropic or axisymmetric turbulence were also conducted in order to compare with sheared cases. The numerical procedure was the same as the one described above for the sheared configuration, with the three directions of the flow being homogeneous.

RESULTS

Several simulations were conducted with the following values of the reference parameters: $Re_r = \frac{\rho_r^* u_r^* L_r^*}{\mu_r^*} = 94$, $M_r = \frac{u_r^*}{c_r^*} = 0.1$, $Pr = 0.7$, where $(\cdot)_r^*$ refers to a dimensional reference variable. The mean Mach number is fixed to $M_1 = 1.5$, and the turbulence parameters in the inflow plane are the following : $Re_\lambda = Re_r\frac{\lambda_{rms}}{\nu} = 47$, $M_t = \frac{q}{\overline{c}} = \frac{\sqrt{\overline{u'_i u'_i}}}{\overline{c}} = 0.173$ and $\chi = 0$. Table 1 summarizes the characteristics of the different runs. They differ by the nature of the mean flow (sheared or not), by the anisotropy of the upstream turbulent flow and by the amount of $\widetilde{u''^2}$ immediately upstream of the shock wave.

Table 1: Characteristics of the different runs. The values reported for the turbulent statistics are taken just before shock.

Run	S	$\widetilde{u''^2}$	$\frac{\widetilde{u''^2}}{q^2}$	$\frac{\widetilde{v''^2}}{q^2}$	$\frac{\widetilde{w''^2}}{q^2}$	$\frac{\widetilde{u''v''}}{q^2}$
SI	1.5	1.04	0.42	0.28	0.31	-0.14
SA1	1.5	1.10	0.44	0.27	0.30	-0.12
SA2	1.5	1.11	0.40	0.29	0.31	-0.17
I	0	1.00	0.35	0.33	0.32	0.005
A1	0	1.04	0.43	0.28	0.30	0.007

Statistics of the flow are gathered when a statistically steady state is established in the computational domain (typically after one flow-through time). Turbulence statistics are then computed by averaging over the homogeneous direction and time. We use 120 instantaneous fields saved during the simulation with a time sampling interval of $2\tau_t/120$, and the total size of the time sample is $2\tau_t$. Apart from the conventional Reynolds average, we shall use Favre's mass-weighted average. For a given function f, it is defined by $\tilde{f} = \overline{\rho f}/\overline{\rho}$, and the corresponding fluctuation is denoted by f''.

Turbulent kinetic energy

Previous works lead to the conclusion that the amplification of the kinetic energy behind the shock wave is strongly dependent of the upstream anisotropic state, and that it is clearly determined by the amount of the longitudinal normal Reynolds stress $\widetilde{u''^2}$ upstream of the shock (see e.g. Jamme *et al.*, 2005). The mean flow was uniform without shear stress is these studies.

In the present work, we first compare three runs (Run SI, Run SA1 and Run SA2) where a mean shear has been introduced. The anisotropy of the turbulence is slightly different just before the shock for these three cases. The near-field amplification of $q^2/2$ behind the shock wave is found to depend on the amount of the correlation $\widetilde{u''T''}$ immediately upstream of the shock. This correlation is positive in the three cases, but its value is not the same. The more $\widetilde{u''T''}$ is high upstream, the less $q^2/2$ is amplified behind the shock (see Figure 2). This effect of $\widetilde{u''T''}$ on the amplification factor of the turbulent kinetic energy through the shock wave has also been highlighted by LIA when the flow is isotropic upstream of the shock wave (Mahesh *et al.*, 1997).

In order to get rid of the effect linked to the amount of $\widetilde{u''^2}$, and trying to isolate the influence of the nature of the anisotropy of the incident turbulent flow itself, we conducted two more runs (Run I and Run A1) in which the amount of $\widetilde{u''^2}$ is the same as in Run SI just before the shock, but not the values of the other components of the Reynolds stress tensor. One can see in Figure 3 that both the axisymmetric and sheared cases show a greater amplification of $q^2/2$ than the isotropic case. Mahesh *et al.* (1996) observed a slight decrease of $q^2/2$ across a $M_1 = 1.2$ shock for a sheared case, and they attributed this trend to the fact that $\widetilde{u''T''} > 0$

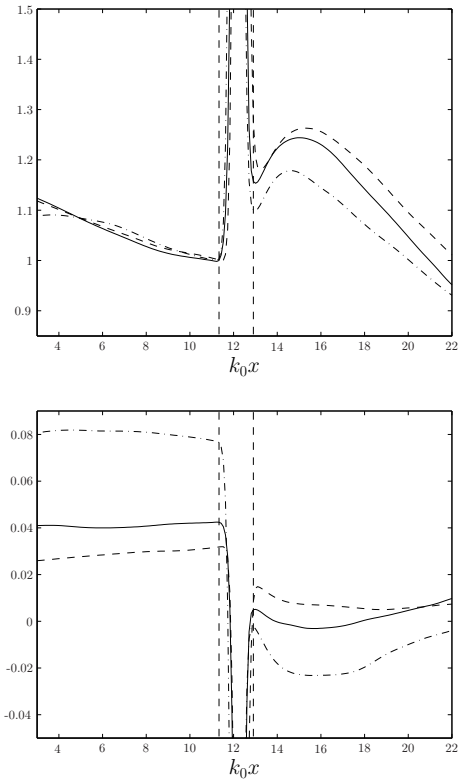

Figure 2: Evolution of $q^2/2$ normalized by its value immediately upstream of the shock wave (up) and $\widetilde{u''T''}$ (down). (——) Run SI ; (– – –) Run SA1 ; (– · –) Run SA2.

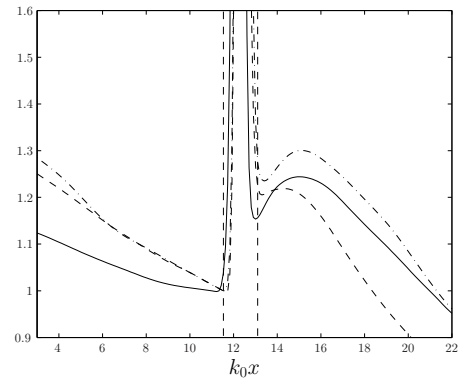

Figure 3: Evolution of $q^2/2$ across the shock, curves are normalized by their value immediately upstream of the shock wave. (——) Run SI ; (– – –) Run I ; (– · –) Run A1.

before the shock, which is known to inhibit the amplification of the kinetic energy. In the present case (Run SI), we have $\widetilde{u''T''} > 0$ upstream ($\widetilde{u''T''} \approx 0.04$ for run SI, whereas it is zero for runs I and A1), but $q^2/2$ is still more amplified in the near field compared to the isotropic situation. This difference with Mahesh *et al.* (1996) may be a consequence of the shock strength ($M_1 = 1.5$ in our case instead of $M_1 = 1.2$).

Reynolds stresses

Figure 4 shows that the axisymmetric case displays a greater near-field amplification of $\widetilde{u''^2}$ than the isotropic case, whereas the opposite is true for the sheared case.

The behaviour of $\widetilde{u''v''}$ is found to be same as the one

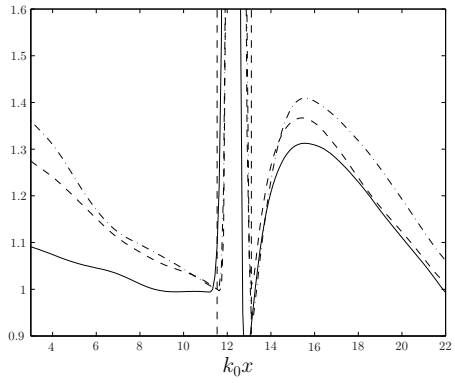

Figure 4: Evolution of $\widetilde{u''^2}$ across the shock, curves are normalized by their value immediately upstream of the shock wave. (——) Run SI ; (– – –) Run I ; (– · –) Run A1.

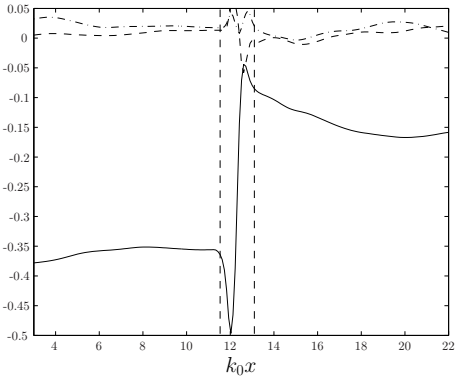

Figure 5: Evolution of $\widetilde{u''v''}$ across the shock. (——) Run SI ; (– – –) Run I ; (– · –) Run A1.

observed by Mahesh *et al.* (1996) : we notice a decrease of the magnitude of $\widetilde{u''v''}$ across the shock wave (see Figure 5). The budget of this quantity is written in Equation (1). This budget is presented in Figure 6. Inside the shock wave (between the vertical dashed lines), coupling terms with the mean flow (production terms (II) and (III)) are negligible. Moreover, pressure-strain correlation (VI) is small compared to pressure-diffusion (V) which is found to be responsible for the decrease in magnitude of $\widetilde{u''v''}$, together with production by the mass-flux fluctuations (IV) and turbulent diffusion (VII). This is in contradiction with the RDT results of Mahesh *et al.* (1994) that attributed the behaviour of $\widetilde{u''v''}$ through the shock wave to the pressure-strain correlation. It should be noticed that in their analysis, neitheir dilatational (compressible) effects nor non-linearities were taken into account.

Behind the shock wave, production by the mean shear (III) displays a constant negative contribution to the budget. This term is in competition with pressure-correlation terms (V) and (VI). In the near-field, these two terms are negative, leading to a rapid decrease of $\widetilde{u''v''}$ just behind the shock. Then the pressure-diffusion term (V) becomes positive so that the decrease of $\widetilde{u''v''}$ becomes smoother. This term vanishes in the far field where the pressure-strain correlation (VI) equilibrates production by the mean shear (III). This equilibrium state (in which $\widetilde{u''v''}$ is constant) is typical of a turbulent homogeneous shear flow. It is also present upstream of the shock, with a higher shear stress than downstream, so that terms (VI) and (III) are more important in magnitude.

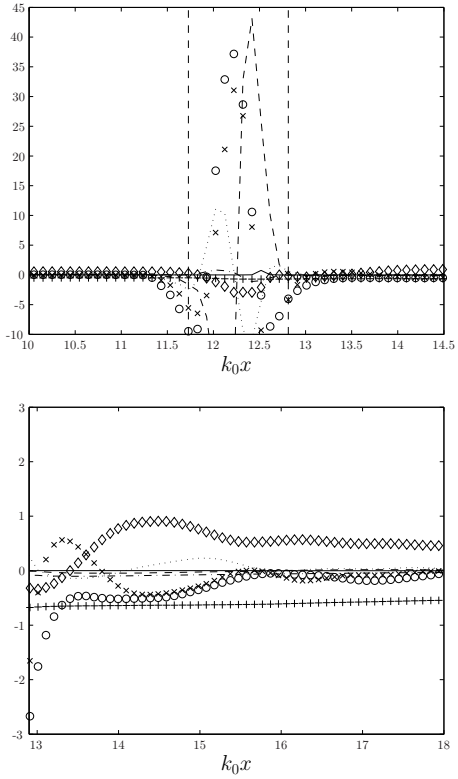

Figure 6: Different terms in the $\widetilde{u''v''}$ budget equation - Run SI - (up) zoom inside the shock zone; (down) evolution downstream of the shock wave. ($\circ\circ\circ$) advection (I); (——) production by the mean compression (II); ($+++$) production by the mean shear (III);($---$) production by the mass-flux fluctuations (IV);($\times\times\times$) pressure diffusion (V); ($\diamond\diamond\diamond$) pressure-strain correlation (VI); ($\cdots\cdots$) turbulent diffusion (VII); ($-\cdot-$) viscous dissipation (VIII).

$$
\underbrace{\overline{\rho}\widetilde{U}\frac{\partial\widetilde{u''v''}}{\partial x}+\overline{\rho}\widetilde{V}\frac{\partial\widetilde{u''v''}}{\partial y}}_{\text{(I)}}=
$$

$$
\underbrace{-\overline{\rho}\widetilde{u''v''}\frac{\partial\widetilde{U}}{\partial x}}_{\text{(II)}}\underbrace{-\overline{\rho}\widetilde{v''^2}\frac{\partial\widetilde{U}}{\partial y}}_{\text{(III)}}\underbrace{-\overline{u''}\frac{\partial\overline{P}}{\partial y}-\overline{v''}\frac{\partial\overline{P}}{\partial x}}_{\text{(IV)}}+ \tag{1}
$$

$$
\underbrace{-\frac{\partial\overline{p'v''}}{\partial x}-\frac{\partial\overline{p'u''}}{\partial y}}_{\text{(V)}}\underbrace{+\overline{p'\left(\frac{\partial u''}{\partial y}+\frac{\partial v''}{\partial x}\right)}}_{\text{(VI)}}
$$

$$
\underbrace{-\frac{\partial}{\partial x}\left(\overline{\rho}u''^2\widetilde{v''}\right)-\frac{\partial}{\partial y}\left(\overline{\rho}u''\widetilde{v''^2}\right)}_{\text{(VII)}}\underbrace{+\overline{u''\frac{\partial\tau_{2k}}{\partial x_k}}+\overline{v''\frac{\partial\tau_{1k}}{\partial x_k}}}_{\text{(VIII)}}
$$

Vorticity

A clear influence of the shear stress can be seen on the streamwise component of the vorticity (cf. Figure 7). An increase of $\overline{\omega_x'^2}$ in the near field behind the shock is indeed observed for the three cases, but this trend is much more pronounced for the sheared case. The vortex stretching by turbulence is found to be responsible for this increase of $\overline{\omega_x'^2}$, which means that this term is enhanced in the sheared case (budgets not shown here).

Concerning the evolution of $\overline{\omega_y'^2}$, Figure 7 shows that the shear effect on the amplification is negligible as we observe the same normalized evolution for all cases. In fact, as it has been shown before (see e.g. Jamme *et al.*, 2002), the mean compression in the budget equation of vorticity is the main contributor for the amplification of $\overline{\omega_y'^2}$ and $\overline{\omega_z'^2}$ across the shock. As a consequence, the shear stress is not involved in this phenomenon. However, we observe that the decay rate of $\overline{\omega_y'^2}$ downstream the shock is lower for the sheared case. Outside the shock zone, the evolutions of $\overline{\omega_x'^2}$ and $\overline{\omega_y'^2}$ depend on the competition between the vortex stretching by turbulence and the viscous term. The increased vortex stretching by turbulence in the sheared case reduces the decay rate of $\overline{\omega_y'^2}$ (and similarly for $\overline{\omega_z'^2}$) compared to the axisymmetric and isotropic situations.

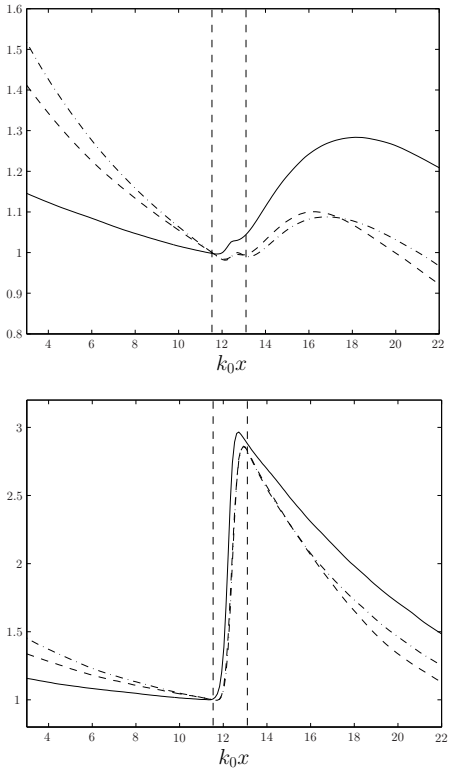

Figure 7: Evolutions of $\overline{\omega_x'^2}$ (up) and $\overline{\omega_y'^2}$ (down) across the shock, curves are normalized by their value immediately upstream of the shock wave. (——) Run SI ; ($---$) Run I ; ($-\cdot-$) Run A1.

Turbulent length scale

Figure 8 displays the evolution of the dissipation length scale $l_\varepsilon = \overline{\rho}q^3/\varepsilon$ which is widely used in turbulence modelling. This scale is found to increase across the shock for the three runs. The amplification factor is not the same for all cases. l_ε is less amplified in the sheared case compared to the isotropic situation, whereas the opposite is true for the axisymmetric run. This amplification of the dissipation length scale is in agreement with previous DNS of isotropic shock-turbulence interaction at Mach 1.5 and LIA results (see Lee *et al.*, 1997).

Thermodynamic fluctuations

Figure 9 shows the variation of the fluctuating density, pressure and temperature during the interaction for run SI. Upstream and far-field downstream states are dominated by temperature and density fluctuations (entropy mode), which

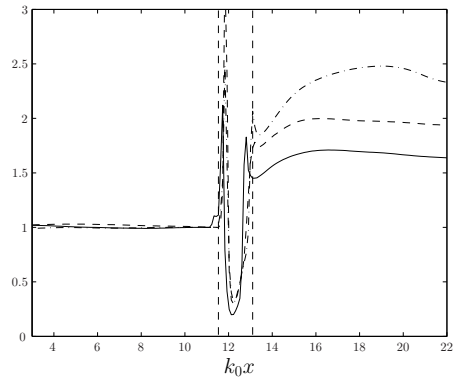

Figure 8: Evolution of l_ε across the shock, curves are normalized by their value immediately upstream of the shock wave. (——) Run SI ; (– – –) Run I ; (– · –) Run A1.

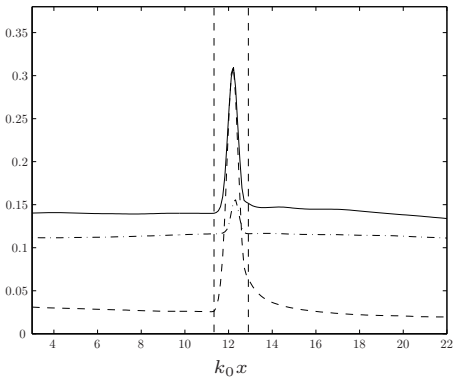

Figure 9: Evolution of rms values of the thermodynamic properties throughout the computational domain, Run SI. (——) $\overline{\rho'^2}/\overline{\rho}$; (– – –) $\overline{p'^2}/\overline{P}$; (– · –) $\overline{T'^2}/\overline{T}$.

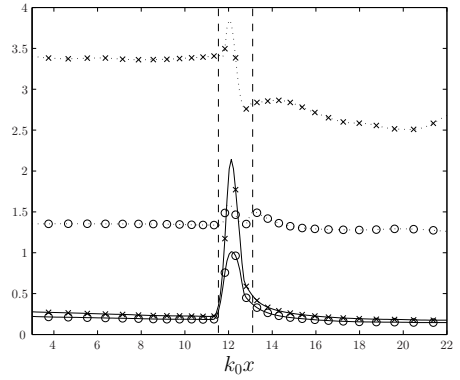

Figure 10: Evolution of the polytropic exponents. (—o—) $n_{p\rho}$ Run SI ; (—×—) n_{pT} Run SI ; (· o · o ·) $n_{p\rho}$ Run I ; (· × · × ·) n_{pT} Run I.

is not true for the isotropic case (run I) where pressure fluctuations dominate. In the sheared case (run SI), pressure fluctuations are enhanced during the interaction but they are negligible except in the near field just behind the shock. Figure 10 displays the polytropic coefficients $n_{p\rho}$ and n_{pT} defined in Equation (2).

$$n_{p\rho} = \frac{\overline{p'^2}/\overline{P}}{\overline{\rho'^2}/\overline{\rho}} \qquad n_{pT} = \frac{\overline{p'^2}/\overline{P}}{\overline{T'^2}/\overline{T}} \tag{2}$$

We can see that thermodynamic fluctuations are isentropic upstream of the shock for the isotropic case (run I), with $n_{p\rho} = \gamma = 1.4$ and $n_{pT} = \gamma/(\gamma - 1) = 3.5$, whereas a slight deviation from the isentropic state is shown downstream. For the sheared case (run SI), the flow is no more isentropic on both sides of the shock. This is due to the presence of a density and temperature gradient in the mean flow (cf. Blaisdell *et al.*, 1993).

CONCLUSION

This work aimed at characterizing the influence of anisotropy of the upstream turbulent flow on shock-turbulence interaction. Several types of anisotropy were considered and combined. We compared the interaction of isotropic, axisymmetric and sheared turbulent flows with a Mach 1.5 shock wave, with a specific interest for the sheared situation. The behaviour of turbulent kinetic energy and Reynolds stresses was first investigated, showing the importance of the sign of the correlation between the velocity and temperature fluctuations on the kinetic energy amplification across the shock. The budget of $\widetilde{u''v''}$ was also reported and allowed to identify the mechanism responsible for the decrease in magnitude of $\widetilde{u''v''}$ observed through the shock wave. Vorticity fluctuations were seen to be affected by the shear stress downstream of the shock, as well as the amplification factor of the turbulent dissipation length scale. Thermodynamic fluctuations were finally analyzed, showing the departure from the isentropic state in the sheared situation compared to the isotropic one.

REFERENCES

Agui, J.H., Briassulis, G. and Andreopoulos Y., 2005, "Studies of interactions of a propagating shock wave with decaying grid turbulence : velocity and vorticity fields", *J. Fluid. Mech.*, Vol. 524, pp. 143-195.

Blaisdell, G.A., Mansour, N.N. and Reynolds W.C., 1993, "Compressibility effects on the growth and structure of homogeneous turbulent shear flow", *J. Fluid. Mech.*, Vol. 256, pp. 443-485.

Fabre, D., Jacquin, L., and Sesterhenn, J., 2001, "Linear interaction of a cylindrical entropy spot with a shock", *Phys. Fluids*, Vol. 13, pp. 2403-2422.

Jamme, S., Cazalbou, J.-B., Torrès, F. and Chassaing, P., 2002, "Direct numerical simulation of the interaction of a shock wave and various types of isotropic turbulence", *Flow, Turbulence and Combustion*, Vol. 68, pp. 227-268.

Jamme, S., Crespo, M. and Chassaing, P., 2005, "Direct numerical simulation of the interaction between a shock wave and anisotropic turbulence," *Proceedings, 35th AIAA Fluid Dynamics Conference and Exhibit*, Toronto, Canada, AIAA Paper 2005-4886.

Jiang, G.-S. and Shu, C.-W., 1996, "Efficient implementation of Weighted ENO schemes", *J. Comp. Phys.*, Vol. 126, pp. 202-208.

Kovasznay, L.S.J., 1953, "Turbulence in supersonic flows", *J. of the Aero. Sci.*, Vol. 20, pp. 657-682.

Lee, S., Lele, S.K., and Moin, P., 1997, "Interaction of isotropic turbulence with shock waves: effect of shock strength", *J. Fluid Mech.*, Vol. 340, pp. 225-247.

Lele, S.K., 1992, "Compact finite difference schemes with spectral-like resolution", *J. Comp. Phys.*, Vol. 103, pp. 16-42.

Mahesh, K., Lele, S.K., and Moin, P., 1994, "The response of anisotropic turbulence to rapid homogeneous one-dimensional compression", *Phys. Fluids*, Vol. 6, pp. 1052-1062.

Mahesh, K., Moin, P., and Lele, S.K., 1996, "The interaction of a shock wave with a turbulent shear flow", Technical Report TF-69.

Mahesh, K., Lele, S.K., and Moin, P., 1997, "The influence of entropy fluctuations on the interaction of turbulence with a shock wave", *J. Fluid Mech.*, Vol. 334, pp. 353-379.

Poinsot, T.J. and Lele, S.K., 1992, "Boundary conditions for direct simulations of compressible viscous reacting flows", *J. Comp. Phys.*, Vol. 101, pp. 104-129.

Ponziani, D., Pirozzoli, S. and Grasso, F., 2003, "Development of optimized Weighted-ENO schemes for multiscale compressible flows", *Int. J. Numer. Meth. in Fluids*, Vol. 42, pp. 953-977.

Ribner, H.S., 1953, "Convection of a pattern of vorticity through a shock wave", Technical Report NACA TN 2864.